




Human Spinal Oligodendrogenic Neural Progenitor Cells Promote Functional Recovery After Spinal Cord Injury by Axonal Remyelination and Tissue Sparing

NARIHITO NAGOSHI,^{a,b,†} MOHAMAD KHAZAEI,^{a,†} JAN-ERIC AHLFORS,^c CHRISTOPHER S. AHUJA,^{a,d,e} SATOSHI NORI,^{a,b} JIAN WANG,^a SHINSUKE SHIBATA,^f MICHAEL G. FEHLINGS^{a,d,e} 

Key Words. Stem cells • Spinal cord injury • Oligodendrogenic neural progenitor cells • Remyelination • Regeneration • Oligodendrocytes

^aDivision of Genetics and Development, Krembil Research Institute, University Health Network, Toronto, Ontario, Canada, ^bDepartment of Orthopaedic Surgery, Keio University School of Medicine, Tokyo, Japan, ^cNew World Laboratories, Laval, Quebec, Canada, ^dInstitute of Medical Sciences, University of Toronto, Toronto, Ontario, Canada, ^eDepartment of Surgery and Spine Program, University of Toronto, Toronto, Ontario, Canada, ^fElectron Microscope Laboratory, Keio University School of Medicine, Tokyo, Japan

[†]Contributed equally.

Correspondence: Michael G. Fehlings, M.D., Ph.D., FRCSC, FACS, University of Toronto, 399 Bathurst St, Toronto Western Hospital, Toronto, Ontario M5T 2S8, Canada. Telephone: 1-416-603-5298, Fax: 1-416-603-5298. E-Mail: michael.fehlings@uhn.on.ca

Received November 17, 2017; accepted for publication June 5, 2018; first published August 7, 2018.

<http://dx.doi.org/10.1002/sctm.17-0269>

This is an open access article under the terms of the Creative Commons Attribution-NonCommercial-NoDerivs License, which permits use and distribution in any medium, provided the original work is properly cited, the use is non-commercial and no modifications or adaptations are made.

ABSTRACT

Cell transplantation therapy utilizing neural precursor cells (NPCs) is a conceptually attractive strategy for traumatic spinal cord injury (SCI) to replace lost cells, remyelinate denuded host axons and promote tissue sparing. However, the number of mature oligodendrocytes that differentiate from typical NPCs remains limited. Herein, we describe a novel approach to bias the differentiation of directly reprogrammed human NPCs (drNPCs) toward a more oligodendrogenic fate (oNPCs) while preserving their tripotency. The oNPCs derived from different lines of human NPCs showed similar characteristics *in vitro*. To assess the *in vivo* efficacy of this approach, we used oNPCs derived from drNPCs and transplanted them into a SCI model in immunodeficient Rowett Nude (RNU) rats. The transplanted cells showed significant migration along the rostro-caudal axis and proportionally greater differentiation into oligodendrocytes. These cells promoted perilesional tissue sparing and axonal remyelination, which resulted in recovery of motor function. Moreover, after transplantation of the oNPCs into intact spinal cords of immunodeficient NOD/SCID mice, we detected no evidence of tumor formation even after 5 months of observation. Thus, biasing drNPC differentiation along an oligodendroglial lineage represents a promising approach to promote tissue sparing, axonal remyelination, and neural repair after traumatic SCI. *STEM CELLS TRANSLATIONAL MEDICINE* 2018;7:806–818

SIGNIFICANCE STATEMENT

Spinal cord injuries (SCI) have devastating physical, social, and financial consequences, and currently lack effective regenerative treatment options. The authors developed a method to generate myelinating oligodendrogenic tripotent neural progenitor cells (oNPCs) directly derived from a patient's own somatic bone marrow cells. Results of this study show a promising approach using oNPCs to replace cells, re-myelinate axons and provide trophic support for tissue sparing, ultimately resulting in functional recovery post-SCI.

INTRODUCTION

Traumatic spinal cord injuries (SCIs) are associated with substantial mortality and long-term morbidity, including loss of functional independence, which underscores the critical need for effective neuroregenerative therapies. At a cellular level, compressive and shearing forces cause laceration, stretching, and mechanical disruption of cell membranes [1–3]. This is followed by a cascade of secondary injury events, which lead to further necrotic and apoptotic loss of neurons and glia over the coming days and weeks. Oligodendrocytes are particularly

susceptible to the cytotoxic conditions within the acute lesion environment, leading to demyelination of neurons and loss of efficient saltatory conduction [4]. Remyelinating white matter tracts by replacing oligodendrocytes represents a promising therapeutic strategy for the treatment of SCI [5, 6].

Neural precursor cells (NPCs) are tripotent cells capable of differentiating into neurons, astrocytes, and oligodendrocytes [7]. Our laboratory and other groups have shown that following traumatic SCI NPCs exert a neuroprotective effect on host cells while also replacing cells from all three neuroglial

lineages [8–11]. However, in most studies, the proportion of engrafted NPCs differentiating to oligodendrocytes is low, especially when utilizing human NPCs. This has been further confirmed both *in vitro* and *in vivo* after transplantation into the rodent central nervous system (CNS) [12, 13]. To improve the potential for transplanted progenitors to differentiate into oligodendrocytes and generate myelin *in vivo*, one approach has been used to transplant oligodendrocyte progenitor cells which are unipotent cells committed to the oligodendrocyte fate [14, 15], or glial-restricted precursor cells which are bipotent cells committed to both an astrocyte and oligodendrocyte fate [16, 17]. However, these strategies fail to replace lost neurons which are also involved in functional recovery, in contrast to NPCs that can replace these cells [18, 19]. Therefore, we sought to bias tripotent human NPCs toward a more oligodendrogenic fate to both preserve the potential for differentiation toward neurons and increase the proportion of oligodendrocytes. Biasing NPCs would increase the proportion of differentiated oligodendrocytes *in vivo* after transplantation while preserving their ability to generate a complement of neurons and astrocytes.

With respect to the cell source for NPCs, numerous studies have intensively focused on induced pluripotent stem cells (iPSCs) [20–23]. iPSCs avoid ethical concerns associated with embryonic stem cells or fetal tissue since they are generated from non-embryonic somatic origin cells. However, recent studies have identified risks associated with iPSC technology, including genetic and epigenetic abnormalities, tumorigenicity, and immunogenicity related to cell transplantation [24, 25]. Therefore, in this study, we focused on drNPCs which were induced from somatic cells. The generation of drNPCs does not involve the pluripotent state, thus making them potentially safer than iPSC-derived grafts [26, 27]. Although mouse-derived directly induced NPCs were assessed as a source for cell transplantation in SCI [28], there have been no studies to evaluate the effectiveness of grafted human drNPCs and their derivatives in the injured spinal cord.

The purpose of this study was to first generate oligodendrogenic-NPCs (oNPCs) efficiently from established human NPC lines, including drNPCs and iPSCs, using our novel method [29]. We next assessed the efficacy and safety of the drNPC-derived oNPCs grafted in a rodent model of SCI. The present study is particularly important as it is the first study to our knowledge which describes human drNPCs biased toward an oligodendrogenic fate for neural repair and regeneration following SCI.

MATERIALS AND METHODS

Human Neural Progenitor Cells

Different lines of hPSCs were used to generate human NPCs using dual SMAD inhibition in monolayer culture [30]. Human iPSC line BC1 was provided by the Centre for Commercialization of Regenerative Medicine (CCRM; Toronto, ON), the hiPSC-P70 was a kind gift from Dr. Andras Nagy (Lunenfeld-Tanenbaum Research Institute, University of Toronto), and ESC line H9 was obtained from WiCell (Wisconsin, MN). All hPSC lines were maintained in feeder free conditions on Matrigel and in mTeSR1.

Human drNPCs were provided by New World Laboratories, Inc. (Laval, QC). drNPCs were directly differentiated from bone marrow somatic cells using transient transfection of the three factors Musashi-1 (Msi1), Neurogenin-2 (Ngn2), and methyl-CpG binding domain protein 2 (MBD2) and defined media containing NeuroCult-XF Proliferation medium (StemCell Technologies; Vancouver, BC) supplemented with epidermal growth factor (EGF) [20 ng/ml] (CellGenix; Freiburg, GER), fibroblast growth factor-2 (FGF-2) [50 ng/ml] (CellGenix), Valproic Acid [VPA, 1 mM] (Sigma-Aldrich; St. Louis, MO), and Noggin [20 ng/ml] (R&D Systems; Minneapolis, MN). VPA and Noggin were replaced by heparin [100 ng/ml] (Scientific Protein Laboratories) after 6 days of culture. Human fetal cortical and spinal NPCs were obtained from Clontech. Different lines of human iPSC-derived, directly reprogrammed or fetal NPCs were cultured and maintained as monolayer on Laminin (8 µg/ml) in NBM-DMEM/F12 (1:1) supplemented with Gluta-max (Life Technologies Cat #10565–018; Waltham, MA), 50% N2 supplement (Life Technologies #175020–01), B27 minus retinoic acid (Life Technologies #12587–010) and FGF (20 ng/ml), EGF (20 ng/ml), and heparin.

Biasing Human NPCs Toward an Oligodendrogenic Fate

We have optimized a general protocol to generate oNPCs from different lines of human PSC-derived, directly reprogrammed or fetal NPCs [29]. The protocol attempts to mimic developmental cues to replicate neural tube patterning *in vitro*. In the first step, the NPCs were caudalized by culturing them on growth factor reduced Matrigel in DMEM/F12, supplemented with 0.1 µM retinoic acid (RA), B27 supplement (Life Technologies, Cat # 17504044), N2 supplement, and EGF (20 ng/ml) for 3 days. Cells underwent ventralization by treatment with 1 µM sonic hedgehog (Shh) agonist Purmorphamine (Millipore, Cat # 540220) for 5 days. EGF was replaced by FGF-2 (10 ng/ml) from the media for 3 days followed by the addition of 20 ng/ml PDGF-AA (Peprotech 100-13A; Rocky Hill, NJ) for 14 days. The resulting cells were maintained on Laminin coated dishes in DMEM/F12, B27-A, N1 supplement (Sigma Cat # N6530), PDGF-AA (20 ng/ml), and FGF-2 (20 ng/ml) for three more passages prior to transplantation. During passaging, 10 µM Rock inhibitor (Y-27632) was added on day 1.

Polymerase Chain Reaction

Cultured NPCs were collected into Buffer RL (Norgen Biotek; Thorold, ON) with β-mercapthenol. Samples were processed according to the manufacturer's directions using a Total RNA Purification Kit (Norgen Biotek—Cat#17200). cDNA synthesis was carried out with SuperScript First-Strand Synthesis System for RT-PCR (Thermo Fisher Scientific—Cat# 11904018). RT-PCR was carried out on GeneAmp PCR System 9700. Cycling conditions consisted of polymerase activation and DNA denaturation (2 minutes at 94°C), followed by 35 cycles of 30 seconds at 94°C, 30 seconds at 58°C, and 60 seconds at 72°C. Values were normalized to the GAPDH housekeeping gene. See the detailed information regarding primer sequences in the Supporting Information Table 1.

Differentiation and Immunocytochemistry

In order to study the differentiation potential of cells *in vitro*, oNPCs were dissociated into single cells and plated on polyornithine/Laminin coated cover glasses (24 well plates:

4×10^3 cells/well). Cells were grown in Neurobasal medium (Thermo Fisher Scientific 21103049; Waltham, MA) supplemented with N2 (Thermo Fisher Scientific 17502048), B27 (Thermo Fisher Scientific 17504044), 0.1% fetal bovine serum, 10 μ M Forskolin (Stem Cell Technologies 72112) and glutamax (Thermo Fisher Scientific 21103049) for an additional 10 days. Cells were fixed for 20 minutes with 4% paraformaldehyde in phosphate-buffered saline (PBS) and 40% sucrose at room temperature. Following fixation, cells were permeabilized in 0.1% Triton X-100 and 0.1% sodium citrate in PBS for 5 minutes and then placed in blocking buffer (5% BSA) for 1 hour. Primary antibodies were diluted in a blocking buffer solution and incubated with the cells overnight at 4°C. Following extensive washing, samples were incubated with DAPI and fluorophore-conjugated secondary antibodies for 1 hour. To quantify, three wells stained for Nestin, β III-Tubulin, GFAP, and O1 were counted within the field of view in five areas within each well. The percentage of differentiated cells was calculated relative to the total numbers of cells in each field of view.

SCI Model

Female RNU rats (athymic nude rats; Crl:NIH-Foxn1^{tmu}; 12-week old; strain code 316; Charles River Laboratories, Wilmington, MA) were used in this study. The clip compression model of SCI has been characterized extensively and described previously [31]. Under inhalational anesthesia using isoflurane (1%–2%) and a 1:1 mixture of O₂/N₂O, the rats underwent a T7–T9 laminectomy and received a 23 g clip (Walsh, Oakville, Ontario, Canada) compression injury for 1 minute at the T7 level of the spinal cord. Gel foam (Ferrosan, Denmark) was put on the spinal cord. Muscles were sutured, and the surgical wound was closed. Their bladders were manually expressed twice daily until the return of reflexive bladder control.

Cell Transplantation in the Spinal Cord

Nine days after injury, the rats were randomly divided into three groups: vehicle (injection of aCSF), control drNPC transplanted, and oNPCs transplanted rats. Ten rats were used per group. Under anesthesia, the spinal cord was reopened at the injury area and the rats were injected with a cell suspension of oNPCs. To prepare the cell suspension, a monolayer culture passage of eight cells was collected using Accutase. The cells were diluted in aCSF and used for cell transplantation. Using a Hamilton syringe connected to a 32-gauge metal needle and a stereotaxic injection system, a total volume of 8 μ l of cell suspension, containing 4×10^5 live cells, was injected into the dorsal spinal cord. We injected the cells into the spinal cord at two sites 2 mm rostral and two sites 2 mm caudal to the lesion area on either side of the midline (0.6–0.8 mm). The injected depth was 0.8–1.0 mm and injection speed was 0.6 μ l/minutes.

Spinal Cord Tissue Processing and Lesion Morphometry

The animals were perfused with 0.1 M PBS, and fixed with 4% paraformaldehyde in the PBS. Postfixation was performed in the same fixative for 6 hours and 30% sucrose in 0.1 M PBS for 24 hours. After fixation, a 1.5 cm length of the spinal cord, centered at the injury site, was collected and sectioned axially at 30 μ m. Serial sections were stained with the myelin-selective stain luxol fast blue (LFB) and hematoxylin and eosin (H&E) as described previously [32]. Unbiased measurements

were made with a Cavalieri volume probe using Stereo Investigator (MBF Bioscience, Williston, VT) for the area of total spinal cord, gray matter, cavity, and total lesion reported. The lesion area was identified as eosinophilic scar deposition with immune infiltrates and/or nonviable or anuclear host tissue [11]. For white matter area quantification, the total area of the total spinal cord was subtracted by the gray matter area and total lesion area. Images were captured at the lesion epicenter and 0.24, 0.48, 0.72, and 0.96 mm rostral and caudal to the epicenter in axial sections.

Immunohistochemistry and Quantification in Spinal Cord Tissue Sections

For immunostaining, the primary antibodies (see Supporting Information) and the appropriate secondary antibodies were used. The images were taken using a Zeiss (Thornwood, NY) LSM 510 laser confocal microscope.

The number of surviving NPCs was assessed by staining with DAPI and anti-HuN on serial spinal cord sections with 240 μ m apart. Under a Leica microscope with $\times 25$ magnification, the areas with HuN⁺ cells were traced on each cross section. Using Stereo Investigator (MicroBrightField Bioscience, Williston, VT), random fields (368 \times 368 μ m), dependent on the size of the transplanted cell area, were imaged under $\times 40$ magnification. Living NPCs (HuN⁺/DAPI⁺) were counted. Considering the thickness of each section and the distance between the slides, the total number of cells was then estimated using the Stereo Investigator.

To quantify Ki67⁺ cells and the proportion of differentiated cell phenotypes in the injured spinal cord, we randomly selected and captured 12 regions within 3,000 μ m rostral and caudal to the lesion epicenter at $\times 63$ magnification (numeric aperture). HuN⁺ transplanted cells and phenotypic marker-positive cells were counted in each region.

Cell Transplantation into the Spinal Cord of NOD/SCID Mice

For the evaluation of safety, we transplanted drNPC-derived oNPCs or control unpatterned drNPCs from the same line as oNPCs (referred to as control NPCs or simply NPCs) into intact spinal cords of NOD/SCID mice (NOD/SCID mice; NOD.CB17-Prkdc^{scid}/NcrCrl) (18–22 g; 8-week old; strain code 394). The mice were anesthetized using isoflurane (1%–1.5%) and 1:1 mixture of O₂/N₂O. The spinal cord was exposed with a T10 laminectomy. A total volume of 4 μ l of cell suspension, containing 2×10^5 live cells, was injected into the dorsal spinal cord. The injection was performed at four sites with 0.5 mm injected depth. To quantify Ki67⁺ cells in transplanted HuN⁺ cells in the intact spinal cord, we randomly selected and captured 12 regions at $\times 63$ magnification (numeric aperture).

Immuno-Electron Microscopy and its Quantification in Spinal Cord Tissue Sections

The detailed procedure for immuno-electron microscopy has been described previously [33]. Briefly, frozen spinal cord axial sections (eight sections derived from each group [drNPCs, oNPCs, and PBS], $n = 3$ mice per group) adjacent to the sections were obtained for the quantification of white/gray matter area. Sections were thawed and incubated with 5% blockage (Dainihon Pharma) in 0.1 M phosphate buffer (PB) with 0.01% saponin for an hour at 25°C, followed by

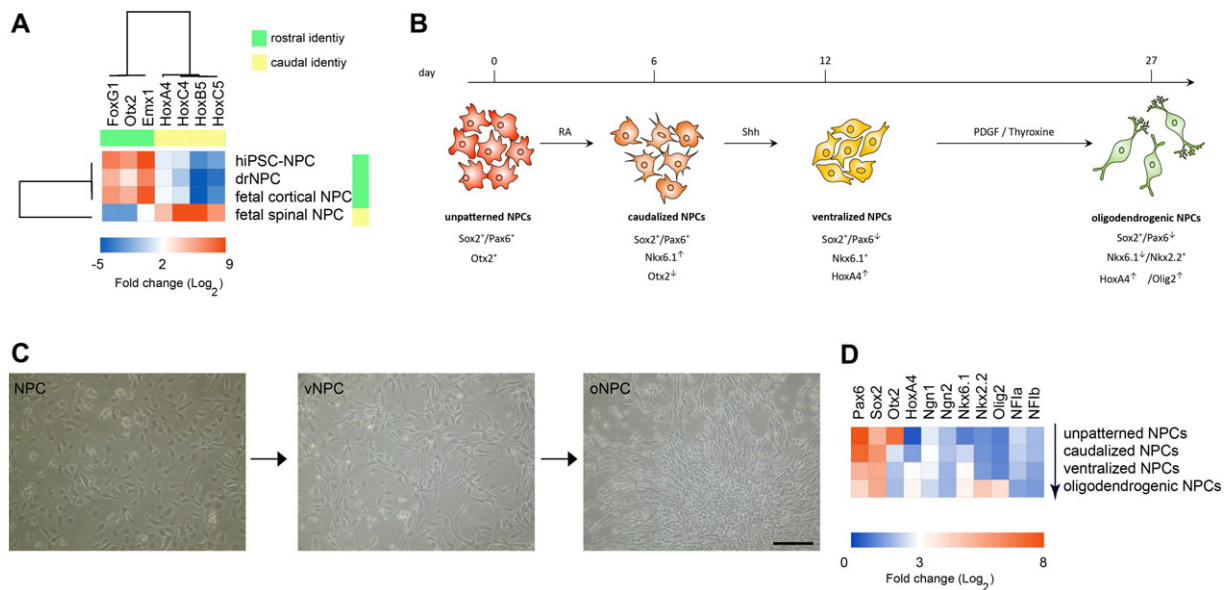


Figure 1. Generation of oligodendrogenic NPCs. **(A):** The gene expression pattern of rostral and caudal identity markers compared between human iPSC-NPCs, drNPCs, fetal cortical NPCs, and fetal spinal NPCs. Hierarchical clustering trees reveal a strong similarity between human iPSC-NPCs, drNPCs, and fetal cortical NPCs while fetal spinal NPCs demonstrated caudal identity. **(B):** Unpatterned NPCs were caudalized using RA and then ventralized by treatment with Shh. To generate oNPCs, these cells were eventually treated with PDGF/thyroxine. **(C):** Gradual changes in the morphology of NPCs after patterning toward oNPCs with elongated mono- and bi-polar morphology. These representative micrographs are from drNPC-derived cells. **(D):** Stepwise changes in the expression profile of NPCs during generation of oNPCs. The expression of transcription factor *Otx2*, an important marker of brain identity, is reduced in caudalized NPCs and they gain the expression of *HoxA4*, a marker of spinal identity in vNPCs. The expression of basic helix loop helix transcription factors *Nkx2.2*, *Olig2*, and *Nkx6.1*, is upregulated in the oNPC stage. Scale bar: 50 μm in (C). Abbreviations: drNPCs, directly reprogrammed human NPCs; iPSC, induced pluripotent stem cell; NPCs, neural precursor cells; oNPCs, oligodendrogenic-NPCs; RA, retinoic acid; vNPCs, ventralized NPCs; Shh, sonic hedgehog.

incubation with mouse anti-human cytoplasm (Stem121) monoclonal antibody (1:200 Takara bio) for 72 hours at 4°C. After washing three times in 0.1 M PB with 0.001% saponin, the sections were incubated with nanogold-conjugated anti-mouse IgG secondary antibody (1:100 Invitrogen) for 24 hours at 4°C. Sections were fixed with 2.5% Glutaraldehyde in 0.1 M PB. HQ-Silver kit was used to enhance the gold signal (Nanoprobes), and the sections were postfixed with 0.5% OsO_4 for 90 minutes, dehydrated through graded ethanol (50%, 70%, 80%, 90%, and 100%), acetone (100%), QY1 (100%), graded Epon (25%, 50%, 75%, and 100%), and embedded into 100% Epon. After complete polymerization for 72 hours at 60°C, ultrathin sections (70 nm thick) were prepared with an ultra-microtome (UC7 Leica), and were stained with heavy metal (uranyl acetate and lead citrate), and observed under a transmission electron microscope (TEM, JEOL 1400plus). One hundred images with gold-labeled transplanted human cells were randomly captured from three independent sections in the epicenter from each group. The averaged diameter of remyelinated axons (100 axons from each group for g-ratio), and remyelination counted in the square area measurement (total 300 axons for myelination frequency) was quantitatively analyzed with the analysis software (TEM center, JEOL).

Basso, Beattie, and Bresnahan Open-Field Locomotion Score

Hind-limb function was tested using the 21-point open-field Basso, Beattie, and Bresnahan (BBB) locomotor scale [34].

www.StemCellsTM.com

Tail-Flick Test

The tail-flick test was performed as a measure of sensory function and allodynia. Animals were wrapped in a soft, dark material to calm them. The dorsal surface of the tail between 4 and 6 cm from the tip was exposed to a beam of light calibrated to 50°C generated from an automated machine (IITC Life Science, Woodland Hills, CA). The timer was stopped when the animal flicked its tail away from the beam of light, indicating an aversive response. Latency was measured at 15-minute intervals over three consecutive trials, with mean latency reported. If animals did not respond to the beam by 20 seconds, the procedure was stopped, and latency was scored as 20.00.

Automated Gait Analysis (CatWalk)

Gait analysis was conducted using the CatWalk system (Noldus Information Technology, Leesburg, VA). Files were collected and analyzed using the CatWalk program, version 10.5. A variety of static and dynamic gait parameters can be measured during locomotion; however, in the present study we analyzed (a) hindlimb stride length (the distance between three consecutive hindlimb paw placements) and (b) hindlimb swing speed (the speed of the paw during the swing phase).

Statistical Analysis

All data are reported as means \pm SEM. For immunohistological and electron microscopic analyses, an unpaired two-tailed Student's *t*-test was used. Histomorphometric and behavioral data were analyzed using two-way repeated-measures analysis of

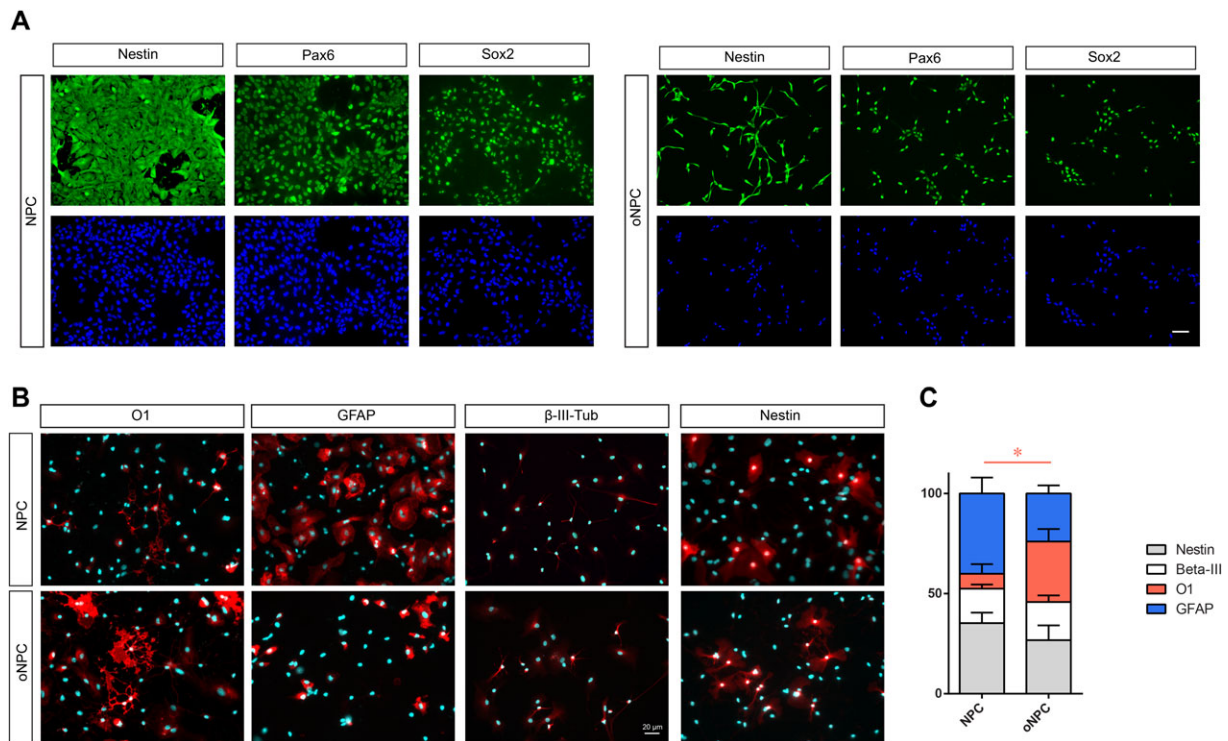


Figure 2. In vitro differentiation profile of oNPCs. **(A):** Both unpatterned NPCs and oNPCs demonstrated comparable expression of neural progenitor markers Pax6, Sox2, and Nestin. The bipolar morphology of oNPCs is evident as compared to NPCs. **(B and C):** Comparison of the differentiation profile of unpatterned NPCs and oNPCs after removal of growth factors epidermal growth factor, basic fibroblast growth factor, and the addition of 0.1% fetal bovine serum. These results and representative micrographs belong to directly reprogrammed human NPCs-derived cells. Results are presented as mean percentage \pm SEM from three independent experiments (average of 10 random fields in each group). * $p < .05$, two-way analysis of variance. Scale bar: 20 μ m. Abbreviations: NPCs, neural precursor cells; oNPCs, oligodendrogenic-NPCs.

variance with Tukey's post hoc tests. The significance level for all analyses was set at $p < .05$.

RESULTS

Human NPCs can be Biased Toward an Oligodendrogenic Fate

First, we investigated whether replicating developmental cues critical to oligodendroglial fate determination could predispose human NPCs to differentiate into oligodendrocytes in proportionally greater numbers. The generation of functional neuroglial subtypes in the vertebrate CNS is a complex process with numerous key steps including the induction of neuroectoderm from embryonic ectoderm, patterning of the neural plate with regional niches along rostrocaudal and dorsoventral axes, and the differentiation of regionalized progenitor cells into post-mitotic neurons and glia [35, 36]. In order to generate oNPCs from human NPCs, we mimicked these exogenous morphogenic cues to replicate neural tube patterning in vitro [29, 37]. To find a consensus patterning protocol, we tested an array of factors across concentrations and time points on four different human NPC lines: fetal cortical NPCs, fetal spinal NPCs, iPSC-derived NPCs, and drNPCs. Both hPSC-NPC and drNPC lines demonstrated a rostral CNS identity, similar to fetal human cortical NPCs, based on their expression levels of Otx2 and FoxG1 (Fig. 1A). Conversely, fetal spinal NPCs demonstrated expression of caudal identity markers (HoxA4, B5, C4, and C5; Fig. 1A).

To caudalize the typically rostral hNPC lines, they were treated with RA, a potent caudalizing factor, for 9 days. From days 6–12, Shh or its agonists were used as ventralizing morphogens to drive hNPCs toward a ventral spinal progenitor fate (Fig. 1B). Fetal human spinal NPCs were only treated with Shh for 6 days. After this time, cells acquired a spinal identity by losing expression of transcription factor Otx2, an important marker of brain identity, and gaining the expression of HoxA4, a marker of spinal identity (Fig. 1D). Cells were treated with PDGF-AA for an additional 2 weeks after which they demonstrated elongated monopolar and bipolar morphologies (Fig. 1C). The resulting cells expressed high levels of basic helix loop helix transcription factors Nkx2.2 and Olig2 (Fig. 1D). The expression of Nkx2.2 and oligodendrogenic transcription factors, such as Olig2 and Nkx6.1, were significantly upregulated in cells at this stage of oNPCs as compared to unpatterned NPCs (Fig. 1D). The expression of neuron-determinant genes Ngn1 and Ngn2 did not significantly change over different stages of biasing, while NF1a and NF1b, two transcription factors involved in astrocyte determination [38], were slightly decreased (Fig. 1D).

oNPCs Generate More Oligodendrocytes In Vitro than Conventional NPCs

We next examined the differentiation of unpatterned NPC and oNPC derivatives in vitro. Both unpatterned NPCs and oNPCs demonstrated comparable expression of neural progenitor markers Pax6, Sox2, and Nestin (Fig. 2A). The bipolar

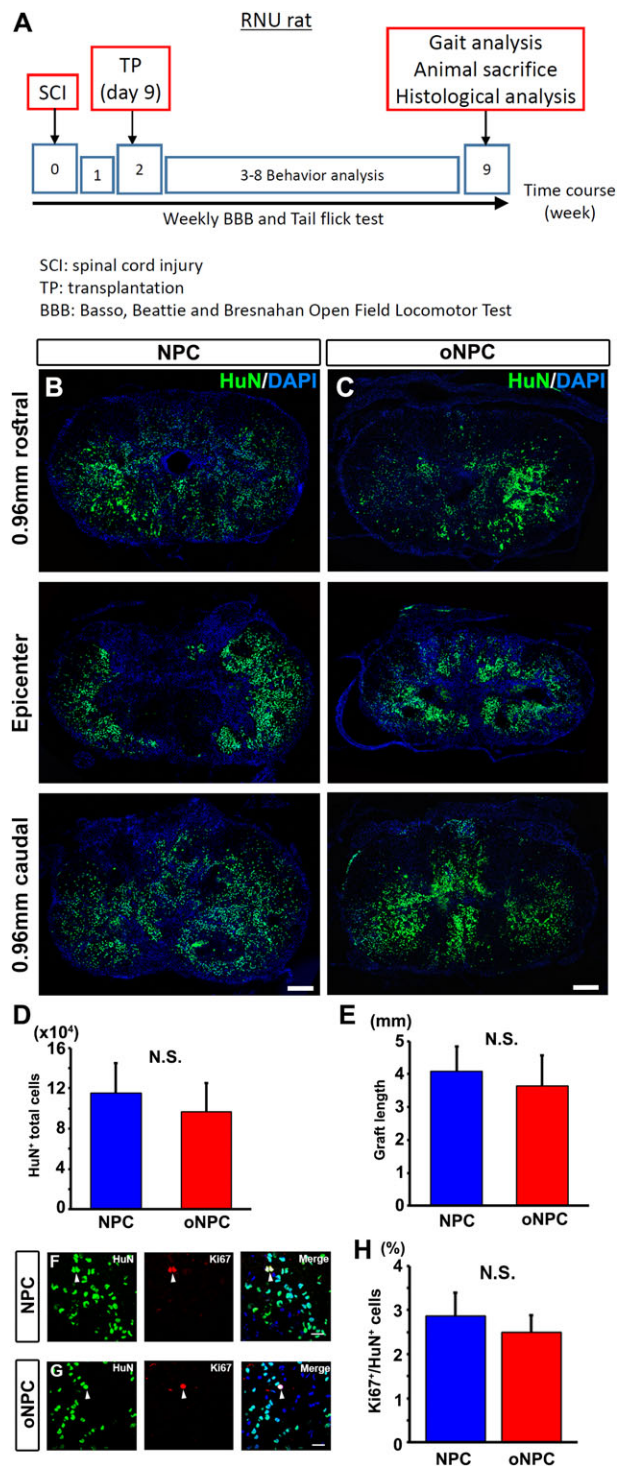


Figure 3. Transplanted oNPCs survive without tumorigenicity. **(A):** A summary of the experimental timeline. **(B and C):** Representative images of the lesion epicenter of the spinal cord, and 0.96 mm rostral and caudal to the site with HuN label. HuN⁺ transplanted directly reprogrammed human NPCs (drNPCs) (B) and drNPC-derived oNPCs (C) dispersed in the tissue and migrated around lesion sites. **(D)** Quantitative analysis of HuN⁺ total cells in the spinal cord ($n = 10$ per each group). **(E):** Quantitative analysis of the transplanted cell distribution as graft length ($n = 3$ per each group). **(F and G):** HuN⁺ cells partially expressed Ki67 (arrowheads). **(H):** Quantitative analysis of Ki67⁺/HuN⁺ cells in the spinal cord ($n = 3$ per each group). Scale bars: 200 μ m in (B and C) and 20 μ m in (F and G). Abbreviations: NPCs, neural precursor cells; oNPCs, oligodendrogenic-NPCs; N.S., not significant; RNU, Rowett Nude.

morphology of oNPCs is evident as compared to NPCs. These oNPCs could be expanded for up to three passages without losing their proliferation and differentiation capacity. After this stage, the proliferation rate of the cells slowed down and they eventually ceased proliferating at passage 5–6, at which point, they morphologically appeared as flat expanded cells. The cell cycle exit and initiation of differentiation was triggered by removal of the growth factors EGF, basic fibroblast growth factor, and addition of 0.1% fetal bovine serum. After 10 days in differentiation conditions, unpatterned hNPCs were characterized by marked process outgrowth, with an increase in the number of processes emanating from the cell body, and extensive branching of these processes. The morphological changes in drNPCs were accompanied by the expression of structural markers characteristic of neuroglial differentiation: astrocytes (GFAP⁺; $40.1 \pm 7.9\%$), neurons (β -III tubulin⁺; $17.2 \pm 2.05\%$), and oligodendrocytes (O1⁺; $7.400 \pm 4.8\%$). The rest of the cells remained in the progenitor stage after 10 days and expressed Nestin (Fig. 2B and 2C). oNPCs cultured in the same differentiation conditions for 10 days displayed a ramified morphology with an intricate lacework of processes that surrounded the cell body. Immunocytochemistry revealed the presence of neurons (β III-tubulin⁺; $19.1 \pm 3.23\%$), but fewer astrocytes (GFAP⁺; $23.95 \pm 4.03\%$) and a significant increase in the numbers of oligodendrocytes (O1⁺; $30.23 \pm 6.22\%$, $p < .5$) demonstrating the multipotency of oNPC and their predisposition for generating oligodendrocytes (Fig. 2C). A portion of oNPCs ($26.7 \pm 7.4\%$) remained in the progenitor stage and expressed Nestin.

oNPCs Migrate and Differentiate Preferentially Toward Oligodendrocytes In Vivo After SCI

To evaluate the efficacy of oNPCs in vivo, we focused on using drNPC derived oNPCs. We transplanted oNPCs 9 days after injury into a clinically-relevant T7 clip-contusion SCI model in T-cell deficient RNU rats (a summary of the experimental timeline is shown in Fig. 3A). As a control group, unpatterned drNPC from the same line of oNPCs were used (hereafter is referred as control NPCs). At 8 weeks post-transplantation, oNPCs were found throughout the spinal cord extending rostrally and caudally from the injury site (Fig. 3B and 3C). The total number of transplanted oNPCs counted by unbiased stereology was 96549.40 ± 28487.19 ($n = 10$), and its ratio was $24.14 \pm 10.07\%$ of the starting population, which was not significantly different from those transplanted with control NPCs ($n = 10$; cell number: 115512.90 ± 29673.44 ; ratio: $28.89 \pm 10.49\%$) (Fig. 3D). The rostral-caudal distribution of grafted cells was also similar between the groups (control NPC: 4.08 ± 0.75 mm; oNPC: 3.65 ± 0.91 mm; $p = .72$; Fig. 3E). The percentage of grafted HuN⁺ expressing Ki67⁺, a marker of proliferation that can be elevated in tumors, was as low as $2.50 \pm 0.38\%$ for oNPCs (number of Ki67⁺ and HNA⁺ cells: 1269.33 ± 161.59 and 54849.67 ± 13087.95) and $2.86 \pm 0.53\%$ for control NPCs (number of Ki67⁺ and HNA⁺ cells: 1445.33 ± 406.82 and 58306.33 ± 21527.87 ; Fig. 3F–3H). The transplanted oNPCs differentiated into all three neuroglial phenotypes in vivo as assessed by β III-tubulin (neurons), GFAP (astrocytes), and APC (mature oligodendrocytes) is shown in Fig. 4. Immunohistochemical analysis showed that, similar to previous reports, some APC⁺ cells also expressed GFAP [39]. Mature oligodendrocytes were identified as APC⁺/

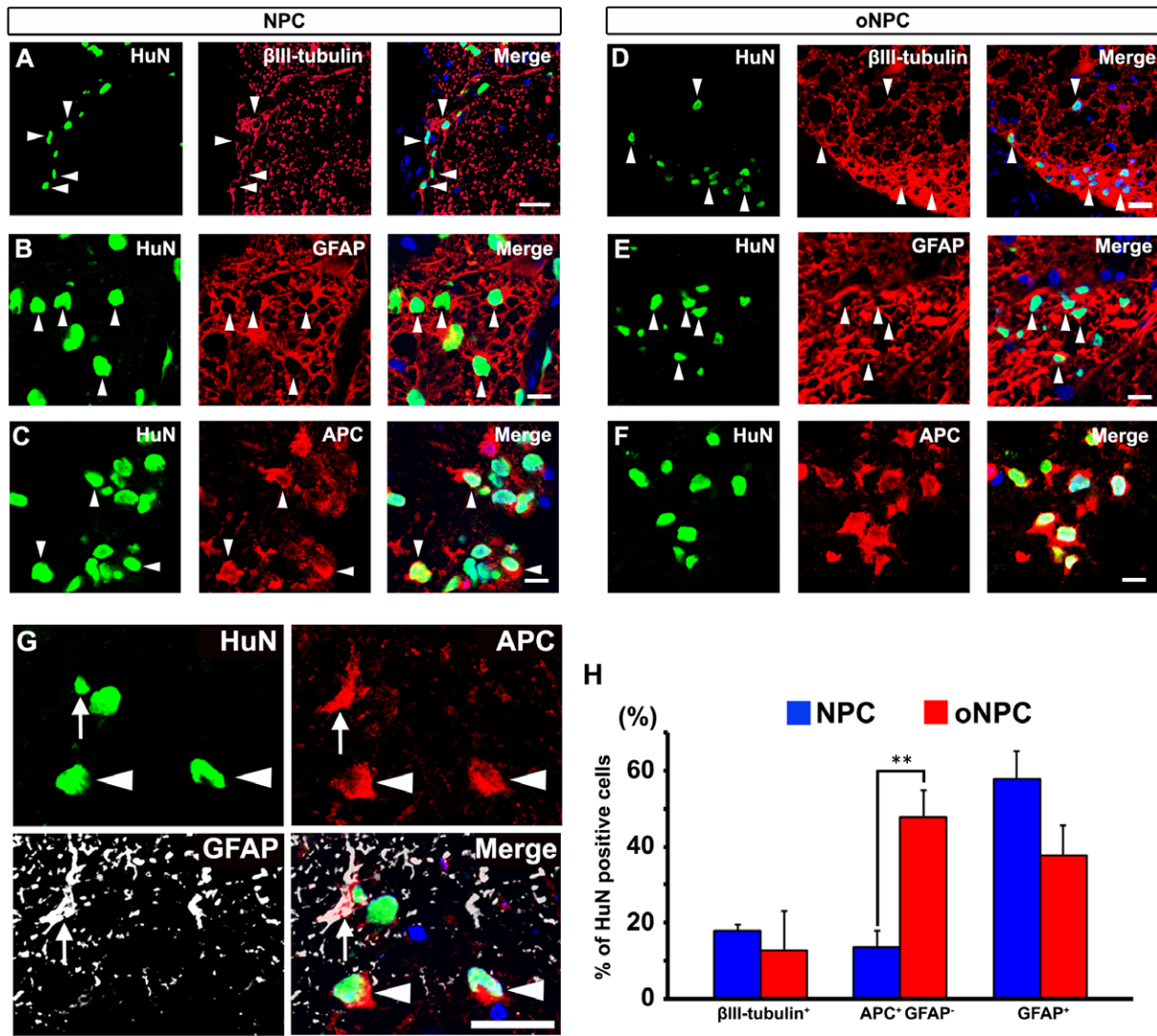


Figure 4. Transplanted oNPCs differentiated into neurons, oligodendrocytes, and astrocytes in the injured spinal cord. (A–F): A representative image of β III-tubulin⁺/HuN⁺ neurons (A and D), GFAP⁺/HuN⁺ astrocytes (B and E; arrowheads), and APC⁺/HuN⁺ cells (C and F). (G): Some of the APC⁺/HuN⁺ cells expressed GFAP (arrow). Oligodendrocytes are APC⁺/GFAP⁻ cells (arrowheads). (H): Quantitative analysis of tri-lineage differentiation profiles with specific markers ($n = 4$ per each group). ** $p < .01$. Scale bar: 25 μ m in (A and D), 20 μ m in (B, C, E, and F), and 10 μ m in (G). Abbreviations: NPCs, neural precursor cells; oNPCs, oligodendrogenic-NPCs.

GFAP⁻ (Fig. 4G). The grafted oNPCs gave rise to significantly greater numbers of oligodendrocytes (APC⁺/GFAP⁻) compared to control NPCs ($47.66 \pm 7.18\%$ vs. $13.63 \pm 4.24\%$; $p < .01$; Fig. 4H).

To analyze the oligodendrocyte-lineage cells differentiated from oNPCs, detailed immunohistochemistry was conducted with several oligodendrocyte markers. The transplanted oNPCs differentiated into Olig2⁺ immature and GST-pi⁺ mature oligodendrocytes (Fig. 5A and 5B). Notably, they expressed MBP which are closely associated with host NF200⁺ axons (Fig. 5C and 5D), indicating the potential of transplanted oNPCs to remyelinate host axons in the injured spinal cord.

To evaluate the distribution of myelin after cell transplantation, electron microscopic examination was performed at the lesion epicenter. In the oNPC group, immature myelin sheaths derived from engrafted human cells (nanogold-labeled Stem121⁺) were frequently observed (Fig. 5E and 5F). In addition, endogenous myelin from host oligodendrocytes was

preserved (Fig. 5E and 5G). The myelination by the control NPC group was not as robust as the oNPC group. The vehicle group showed only a few myelinated axons at the lesion site (Fig. 5I). To evaluate the potential for myelination by grafted cells, we analyzed g-ratios for axons in both the NPC and oNPC groups (Fig. 5J). This analysis revealed that the regression coefficient (in plots of g-ratio vs. axonal diameter) was significantly smaller in the oNPC group compared with the one in the NPC group (0.051 vs. 0.089 , $p < .01$), suggesting that the transplanted oNPCs had more active ability to myelinate host axons. In addition, the average number of myelinated axons per field was significantly larger in the oNPC group, derived from both grafted cells with characteristics of attachment of nanogold dots (1.85 ± 0.27 vs. 0.55 ± 0.12 , $p < .01$ in Fig. 5K) and endogenous cells without the dot attachment (4.28 ± 0.71 vs. 1.40 ± 0.28 , $p < .01$ in Fig. 5L). Therefore, similar to what was observed in vitro, oNPCs generated myelinating oligodendrocytes following transplantation in vivo, and also preserved

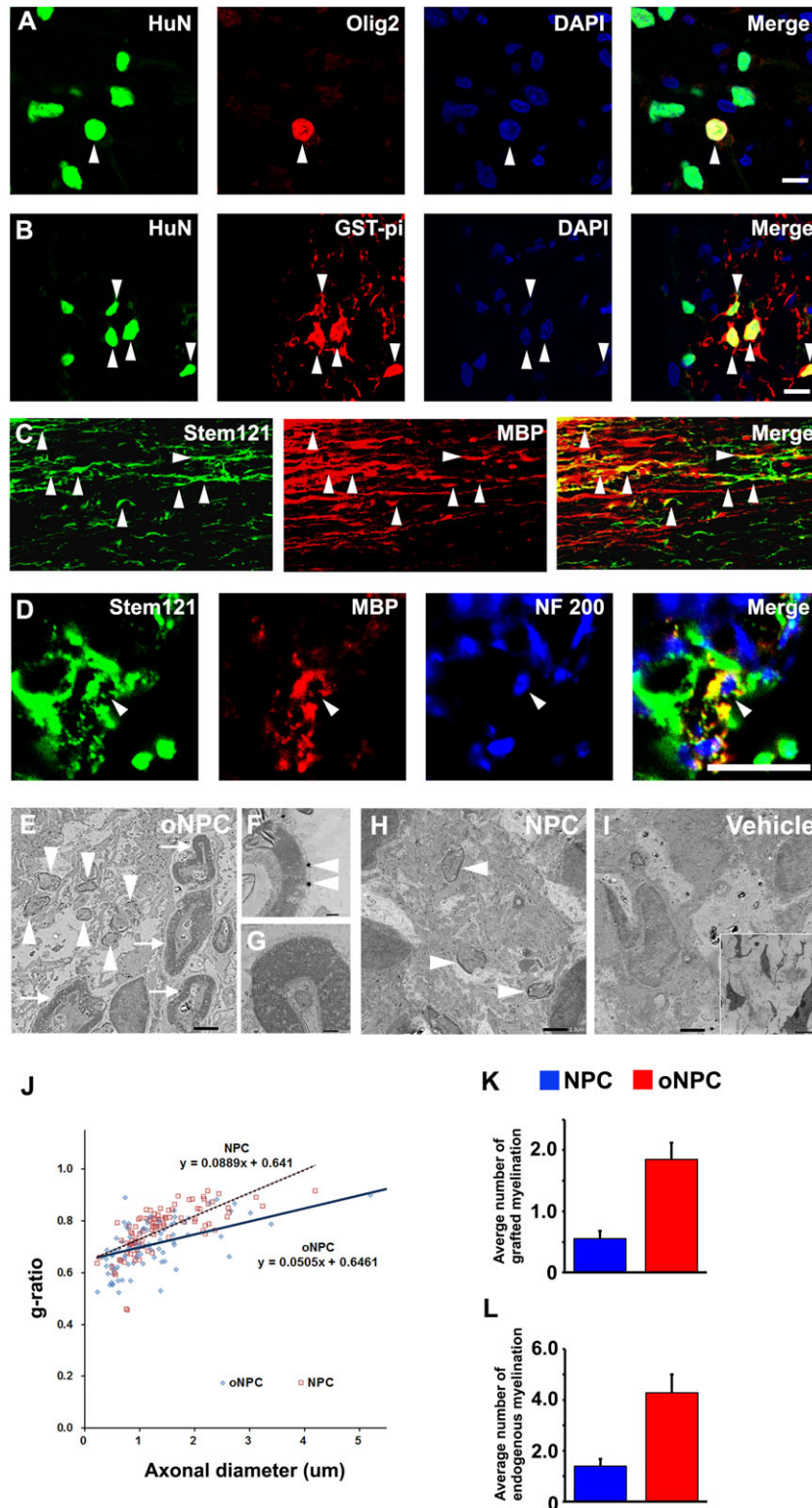


Figure 5.

endogenous oligodendrocytes with spared axons in comparison with NPCs.

Given the EM findings demonstrating that oNPCs promote the generation of new myelin and sparing of endogenous

myelin, we next performed a histomorphometric analysis of the preserved tissue and lesion volume analysis. LFB- and H&E-staining was examined 9 weeks after SCI (Fig. 6A). The white matter area was significantly larger in the oNPC group

compared to the other groups at the lesion epicenter, and extending rostrally and caudally along the neuraxis (Fig. 6B). There was no significant difference in the size of the gray matter or cavity area among the groups (Fig. 6C and 6E). However, the lesion area was significantly reduced at the epicenter in the oNPC group (Fig. 6D). Therefore, the transplanted oNPCs contributed to white matter sparing and reduced lesion volume at 8 weeks post-transplantation.

Improvement of Motor Function Without Allodynia After oNPC Transplantation

We evaluated locomotor coordination and trunk stability using the BBB open-field locomotion scale. BBB scores showed significantly improved functional recovery after SCI in the oNPC group compared to the vehicle group (weeks 7–9; $p < .05$) (Fig. 7A). Further, we conducted gait analysis using the CatWalk Digital Gait Analysis system (Noldus, Inc.; Fig. 7B). Gait analysis revealed that oNPC transplanted rats had significantly better recovery in terms of stride length and swing speed relative to the vehicle and control NPC group (Fig. 7C and 7D). To determine whether sensory impairments occurred following cell transplantation, the tail-flick test was used to measure thermal allodynia. Notably, we found no significant difference between groups, suggesting that the transplanted cells did not contribute to postinjury sensory dysfunction (Fig. 7E).

oNPC Transplantation is not Associated with Tumor Formation In Vivo After Long-Term Follow-Up

To evaluate the tumorigenicity of oNPCs, we transplanted cells into the intact spinal cords of NOD/SCID mice ($n = 3$) and observed them over 150 days. The mice appeared healthy with no overt neurological deficits during the observational period. At 150 days post-transplantation, a histological analysis was conducted with immunohistochemistry for Ki67 and HuN showing colocalization in only $0.94 \pm 0.47\%$ of HuN⁺ cells in the cord (Supporting Information Fig. S1B and S1D). A subpopulation of the transplanted cells expressed Nestin, a marker for undifferentiated neural cells, but the distribution was sparse and tumor-like masses were not observed (Supporting Information Fig. S1E and S1F). Moreover, H&E staining was performed at the injection site of cell transplantation, and formation of neural rosettes was not detected (Supporting Information Fig. S1G and S1H).

DISCUSSION

After SCI, all neural cell types (neurons, oligodendrocytes, and astrocytes) are subjected to cell death. Thus, we would anticipate that ideal cell replacement for traumatic SCI therapy would replace all neural cell types. As the host microenvironment plays an important role in fate determination of engrafted cells, the level of maturation and differentiation of cells at the time of transplantation is another critical factor determining their fate and integration. In the post injury niche, most transplanted NPCs tend to differentiate to astrocytes, and to a lesser extent neurons, while the proportion of oligodendrocytes is very low. To address this, we biased the differentiation profile of NPCs toward more oligodendrocytes rather than astrocytes. This study generates a novel tripotent human NPC, which has been biased prior to transplant toward an oligodendrogenic fate, and assesses its efficacy in a highly clinically relevant contusion-compression model of T-cell deficient rodent thoracic SCI.

Previous studies have demonstrated that transplantation of oligodendrogenic cells can promote tissue repair and functional recovery [15, 40]. The post-transplanted oligodendrocyte progenitor cells derived from ESCs or iPSCs at the subacute stage have been shown to promote white matter preservation, along with an increased number of surviving endogenous oligodendrocytes and reduced cavity volume, resulting in enhanced functional motor recovery [41–43]. The underlying mechanism in these studies was remyelination, local immunomodulation, trophic support, and environmental conditioning through the provision of a physical scaffolding for elongating axons. The current study builds on these results and revealed that cells derived from transplanted oNPCs are capable of remyelinating host axons and generating new neurons. Furthermore, engrafted oNPCs migrated throughout the lesional and perilesional regions, reduced the total lesional area, and increased white matter volumes due to differentiation of myelinating oligodendrocytes and preservation of host tissues. The enhanced myelination was observed to correlate with improved motor recovery and trunk stability in behavioral assessments.

In this study, significant restoration of motor function was observed at 7 weeks after SCI. However, beneficial effects were observed starting at 2 weeks, which could be earlier than the timing typically observed for maturation of myelination. In accordance with our results, previous studies that transplanted human oligodendrogenic NPCs observed beneficial motor recovery effects at 3–6 weeks postinjury [42, 43]. This early

Figure 5. oNPCs predominantly differentiated into oligo-lineage cells and myelinated host axons. **(A–D):** Representative images of Olig2⁺/HuN⁺ immature (A) and GST-pi⁺/HuN⁺ mature (B) oligodendrocytes (arrowheads). The transplanted Stem121⁺ cells colocalized with MBP at sagittal section (C; arrowheads), and there were MBP⁺/Stem121⁺ mature oligodendrocytes myelinating host NF 200⁺ neuronal axons at axial section (D; arrowheads). These cells mainly existed in the white matter area of the spinal cord. **(E–I):** Representative images of immunoelectron microscopy in oNPCs (E–G), NPC (H), and vehicle groups (I). Grafted cells were detected by the black dots observed upon anti-Stem121 antibody staining. Note that myelination with and without attachment of nanogold particles was identified as being attributed to oligodendrocytes derived from transplanted cells (E; arrowheads, F) and endogenous oligodendroglially-mediated myelination with thicker lamellar structure (E; arrows, G), respectively. At higher magnifications in the oNPC group, remyelinated axons surrounded by transplanted cells were identified with characteristic attachment of black dots (F, arrowheads), and endogenous myelin from oligodendrocytes was preserved (G). Arrowheads and arrows indicate myelin derived from transplanted cells and endogenous cells, respectively. **(J):** Regression analysis for plots of g-ratio versus axonal diameter at lesion epicenter. **(K and L):** The average number of myelinated axons derived from grafted cells (K) and endogenous cells (L) per field at lesion epicenter by electron microscopic examination ($n = 3$ per each group). Scale bar: 10 μm in (A, B, and D), 50 μm in (C), 2 μm in (E, H, and I), 5 μm in (small square in I), and 200 nm in (F, G). Abbreviations: NPCs, neural precursor cells; oNPCs, oligodendrogenic-NPCs.

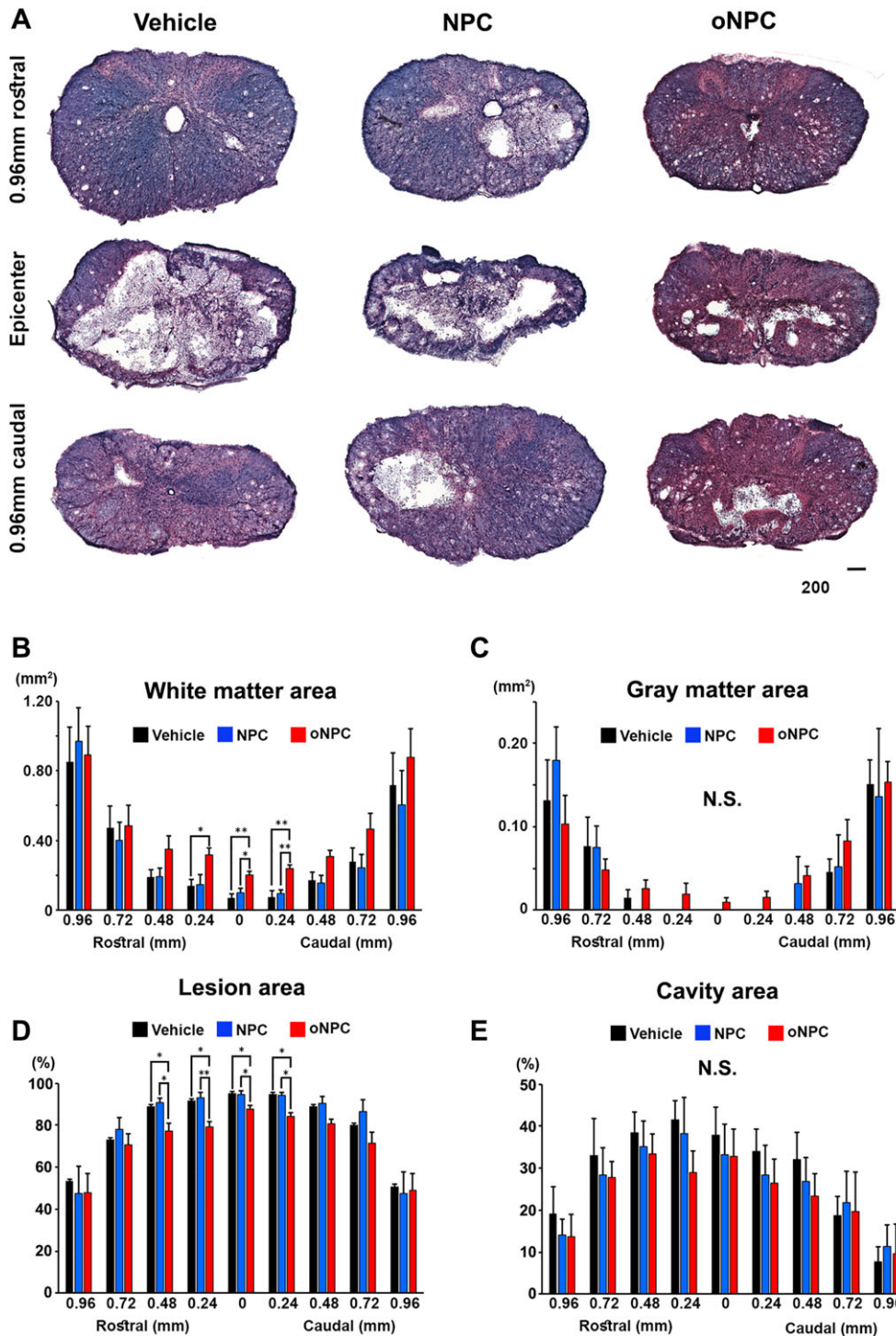


Figure 6. Histomorphometric analysis using luxol fast blue and hematoxylin and eosin staining. **(A):** Representative images of the spinal cord at lesion epicenter and 0.96 mm rostral and caudal area in vehicle, directly reprogrammed human NPCs (drNPC)-derived oNPC (oNPC) and unpatterned drNPC (control NPC) groups. Scale bar: 200 μ m. **(B):** Calculation of white matter area between 0.96 mm rostral and caudal from epicenter. Note that significantly larger white matter area was observed in the oNPCs group around the epicenter area, compared to the other groups. **(C):** Calculation of gray matter area. **(D):** Quantitative analysis of percentage of lesion area/total spinal cord area. Note that a significant reduction of lesion area was observed around the epicenter in the oNPC group. **(E):** Quantitative analysis of percentage of cavity area/total spinal cord area. All analyses were conducted with six rats per group. * $p < .05$; ** $p < .01$. Abbreviations: NPCs, neural precursor cells; N.S., not significant; oNPCs, oligodendrogenic-NPCs.

recovery mechanism could be explained by neurotrophic factors, because past research has revealed that oligodendrocyte-lineage cells, such as immature oligodendrocyte progenitor cells or their derivative mature oligodendrocytes, secreted

neurotrophic factors, such as brain-derived neurotrophic factor, glial cell-derived neurotrophic factor, and neurotrophin-3 [44, 45]. These factors play an important role in enhancing neuronal survival and promoting oligodendrocyte myelination,

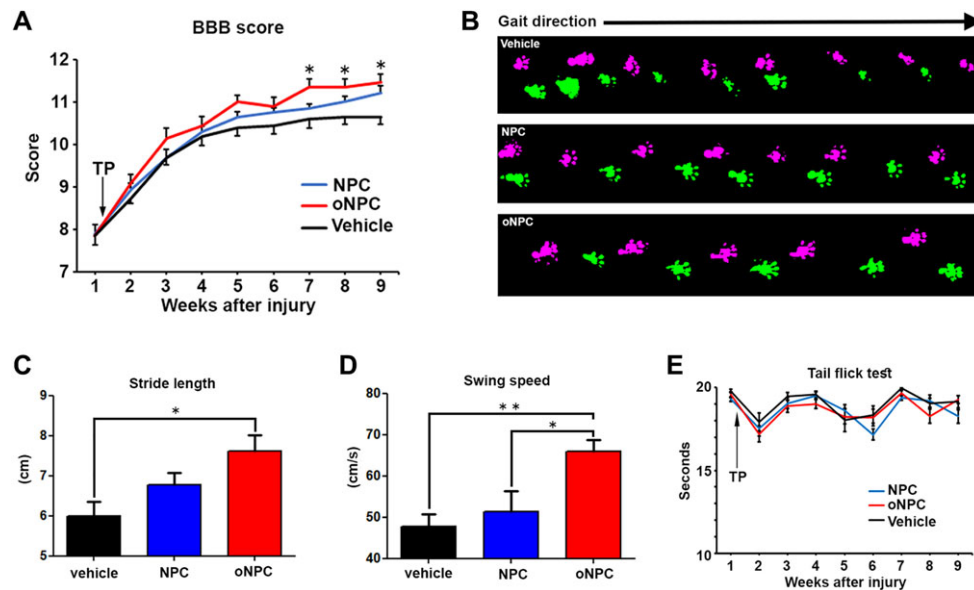


Figure 7. Functional analysis following cell transplantation. **(A):** Time course of motor functional recovery of hindlimbs in BBB score. Rats with oNPCs transplantation showed significant recovery from 7 to 9 weeks after spinal cord injury (SCI). **(B):** Representative images of gait analysis with CatWalk system 9 weeks after SCI. Pink and green footprints indicate right and left hindlimbs, respectively. **(C and D)** Gait analysis with the CatWalk system. Note that there was significantly better recovery in stride length between the oNPC and vehicle groups, and swing speed in the oNPC group compared to the other groups. **(E):** Evaluation of thermal allodynia in the tail-flick test. In each test, 10 rats per each group were examined. * $p < .05$; ** $p < .01$. Abbreviations: BBB, Basso, Beattie, and Bresnahan; NPCs, neural precursor cells; oNPCs, oligodendrogenic-NPCs; TP, transplantation.

which both lead to neuronal protection. Although we did not examine the secretion of these factors from our cultured NPCs, the trophic support mechanism of transplanted cells might contribute to the recovery of locomotor function at this early stage.

The entire reprogramming process to generate human drNPCs is shorter in duration than the process to generate iPSC-derived NPCs [46]. This represents a significant advantage for using these cells because optimal timing for cell transplantation is around 1 month after SCI in primates at the subacute phase [47]. Thus, this process represents a feasible approach to induce and transplant autologous directly reprogrammed cells originating from the patient's own somatic cells in a realistic time frame and decreasing the chance of rejection and increasing the survival of transplants. Since our transplanted drNPC-derived oNPCs showed effective and safe properties in the injured spinal cord, future work should focus on improving the induction and culture protocols, with the end goal of clinical application.

The *in vivo* differentiation profile of conventional NPCs in SCI typically consists of approximately 80% astrocytes, which are associated with increased allodynia [48]. Although they used rodent NPCs and their results could not be directly compared with ours, *in vitro* pro-oligodendrogenic conditioning of hNPCs in our study can substantially reduce the number of resultant astrocytes 9 weeks after transplant. Consequently, we did not detect a significant increase in allodynia by tail-flick test in the animals that received transplants.

Transplantation of iPSC-NPCs requires particular attention to risks associated with iPSC-derived cells, namely tumor formation. We demonstrated the safety of the oNPCs by grafting them into injured rodent spinal cords and finding no morphological or marker-based ($Ki67^+$ percentage: $2.50 \pm 0.38\%$) evidence of

neoplastic transformation. Furthermore, after transplant of oNPCs into intact spinal cords of immunodeficient NOD/SCID mice, we observed no evidence of tumor formation after 5 months of observation with a ratio of $Ki67^+$ transplanted cells of $0.97 \pm 0.47\%$. Although pathological condition (injury or intact) and animal species (rat or mouse) were different, these temporal data might indicate that cell division of the transplants gradually decreased over time. Moreover, our histological analysis using Nestin in NOS/SCID mice showed sparse distribution of transplanted cells, without formation of tumor-like masses (Supporting Information Fig. S2E and S2F). In the same mice, we did not detect any formation of neural rosettes using H&E staining (Supporting Information Fig. S2G and S2H). While there is no standard definition of the tumor forming potential of transplanted cells, our analysis of proliferation, undifferentiation, and the lack of tumor-like masses (as revealed by histological analysis) at 150 days suggest that the oNPCs have considerable clinical potential with no overt safety concerns.

A recently established preclinical grading system proposed that rat models of SCI are more clinically relevant than mouse models [49]. Unlike mouse models, rat models exhibit extensive cavity formation in the chronic injury phase, which closely resembles the pathophysiology of human SCI. Tests of motor function and gait are also well validated for rats. For this reason, we utilized a clinically relevant clip-contusion T7 SCI model using athymic RNU rats. These rats are T-cell deficient, which allowed for enhanced xenograft survival for longer periods without the need for repeated, invasive injections of immunosuppressants. As a result, the animals tolerated the SCI surgeries and postoperative care very well, leading to reduced animal attrition compared to other published studies. Additionally, the survival of transplanted cells at the

completion of the study was 24%, which is dramatically higher than the rates in studies using immunocompetent animals with immunosuppressants [50].

The current study has a few limitations that should be discussed. First, we transplanted cells in the subacute phase of SCI. Given that many patients are in the chronic phase of their injuries, future preclinical studies should evaluate the efficacy of oNPC transplantation in the chronic phase, combined with modifying the chronic environment [51]. Similarly, while it is likely that findings from this thoracic study will extend to other spinal cord regions such as the cervical spine, this must be assessed in a follow-up study [52]. Second, we only transplanted oNPCs derived from a single parent line of hNPCs; however, variation in differentiation and response to the injury microenvironment between different cell lines may exist. Thus, future studies are needed to confirm our findings across different cell sources. Finally, with respect to safety, moving toward translation will require longer observation periods to further assess tumorigenicity and the application to additional large animal species. Moreover, genomic and epigenomic stability should be evaluated to further assess safety.

CONCLUSION

We report that human drNPC-derived oNPCs are an exciting therapeutic option to regenerate the traumatically injured spinal cord with clear evidence of efficacy and data suggestive of safety in vivo.

REFERENCES

- Baptiste DC, Fehlings MG. Pharmacological approaches to repair the injured spinal cord. *J Neurotrauma* 2006;23:318–334.
- Rowland JW, Hawrylyk GWJ, Kwon B et al. Current status of acute spinal cord injury pathophysiology and emerging therapies: Promise on the horizon. *Neurosurg Focus* 2008;25:E2.
- Tator CH, Duncan EG, Edmonds VE et al. Changes in epidemiology of acute spinal cord injury from 1947 to 1981. *Surg Neurol* 1993;40:207–215.
- Li GL, Farooque M, Holtz A et al. Apoptosis of oligodendrocytes occurs for long distances away from the primary injury after compression trauma to rat spinal cord. *Acta Neuropathol (Berl)* 1999;98:473–480.
- Tetzlaff W, Okon EB, Karimi-Abdolrezaee S et al. A systematic review of cellular transplantation therapies for spinal cord injury. *J Neurotrauma* 2011;28:1611–1682.
- Trounson A, McDonald C. Stem cell therapies in clinical trials: Progress and challenges. *Cell Stem Cell* 2015;17:11–22.
- Ladran I, Tran N, Topol A et al. Neural stem and progenitor cells in health and disease. *Wiley Interdiscip Rev Syst Biol Med* 2013;5:701–715.
- Barnabé-Heider F, Frisén J. Stem cells for spinal cord repair. *Cell Stem Cell* 2008;3:16–24.
- Salewski RP, Mitchell RA, Li L et al. Transplantation of induced pluripotent stem cell-derived neural stem cells mediate functional recovery following thoracic spinal cord injury through remyelination of axons. *STEM CELLS TRANSLATIONAL MEDICINE* 2015;4:743–754.
- Tsuji O, Miura K, Okada Y et al. Therapeutic potential of appropriately evaluated safe-induced pluripotent stem cells for spinal cord injury. *Proc Natl Acad Sci USA* 2010;107:12704–12709.
- Wilcox JT, Satkunendrarajah K, Zuccato JA et al. Neural precursor cell transplantation enhances functional recovery and reduces astrogliosis in bilateral compressive/contusive cervical spinal cord injury. *STEM CELLS TRANSLATIONAL MEDICINE* 2014;3:1148–1159.
- Jakovcevski I, Filipovic R, Mo Z et al. Oligodendrocyte development and the onset of myelination in the human fetal brain. *Front Neuroanat* 2009;3:5.
- Budday S, Steinmann PI, Kuhl E. Physical biology of human brain development. *Front Cell Neurosci* 2015;9:257.
- Sharp J, Frame J, Siegenthaler M et al. Human embryonic stem cell-derived oligodendrocyte progenitor cell transplants improve recovery after cervical spinal cord injury. *STEM CELLS* 2010;28:152–163.
- Faulkner J, Keirstead HS. Human embryonic stem cell-derived oligodendrocyte progenitors for the treatment of spinal cord injury. *Transpl Immunol* 2005;15:131–142.
- Cao Q, Xu XM, Devries WH et al. Functional recovery in traumatic spinal cord injury after transplantation of multilineurotrophin-expressing glial-restricted precursor cells. *J Neurosci* 2005;25:6947–6957.
- Gregori N, Pröschel C, Noble M et al. The tripotential glial-restricted precursor (GRP) cell and glial development in the spinal cord: Generation of bipotential oligodendrocyte-type-2 astrocyte progenitor cells and dorsal-ventral differences in GRP cell function. *J Neurosci* 2002;22:248–256.
- Kadoya K, Lu P, Nguyen K et al. Spinal cord reconstitution with homologous neural grafts enables robust corticospinal regeneration. *Nat Med* 2016;22:479–487.
- Fujimoto Y, Abematsu M, Falk A et al. Treatment of a mouse model of spinal cord injury by transplantation of human induced pluripotent stem cell-derived long-term self-renewing neuroepithelial-like stem cells. *STEM CELLS* 2012;30:1163–1173.
- Takahashi K, Tanabe K, Ohnuki M et al. Induction of pluripotent stem cells from adult human fibroblasts by defined factors. *Cell* 2007;131:861–872.
- Kobayashi Y, Okada Y, Itakura G et al. Pre-evaluated safe human iPSC-derived neural stem cells promote functional recovery after spinal cord injury in common marmoset

ACKNOWLEDGMENTS

We thank Dr. Paul Bradshaw for critical reading of the manuscript and comments and Jonathon Chio for assisting with LFB and H&E staining. This study was supported by an Industry Sponsored Collaborative Research Grant with New World Laboratories, Inc. and the Canadian Institutes of Health Research (CIHR). C.S.A. is supported by fellowship funding from CIHR. M.G.F. is supported by the Gerry and Tootsie Halbert Chair in Neural Repair and Regeneration and by grant support from the Dezwirek Foundation and the Krembil Foundation. J.E.A. is CEO and CSO of New World Laboratories Fortuna Fix.

AUTHOR CONTRIBUTIONS

N.N. and M.K.: conception and design, collection and/or assembly of data, data analysis and interpretation, manuscript writing, final approval of manuscript; J.-E.A.: conception and design, provision of study material or patients; C.S.A.: collection and/or assembly of data, manuscript writing, final approval of manuscript; S.N., J.W., and S.S.: collection and/or assembly of data; M.G.F.: conception and design, collection and/or assembly of data, provision of study material or patients, data analysis and interpretation, final approval of manuscript, financial support.

DISCLOSURE OF POTENTIAL CONFLICTS OF INTEREST

J.E.A. declared employment and stock ownership with New World Laboratories and Fortuna Fix. The other authors indicated no potential conflicts of interest.

without tumorigenicity. *PLoS One* 2012;7:e52787.

22 Lu P et al. Long-distance axonal growth from human induced pluripotent stem cells after spinal cord injury. *Neuron* 2014;83:789–796.

23 Nori S, Okada Y, Itakura G et al. Grafted human-induced pluripotent stem-cell-derived neurospheres promote motor functional recovery after spinal cord injury in mice. *Proc Natl Acad Sci USA* 2011;108:16825–16830.

24 Nori S, Okada Y, Nishimura S et al. Long-term safety issues of iPSC-based cell therapy in a spinal cord injury model: Oncogenic transformation with epithelial-mesenchymal transition. *Stem Cell Rep* 2015;4:360–373.

25 Yu DX, Marchetto MC, Gage FH. Therapeutic translation of iPSCs for treating neurological disease. *Cell Stem Cell* 2013;12:678–688.

26 Chanda S, Ang CE, Davila J et al. Generation of induced neuronal cells by the single reprogramming factor ASCL1. *Stem Cell Rep* 2014;3:282–296.

27 Pang ZP, Yang N, Vierbuchen T et al. Induction of human neuronal cells by defined transcription factors. *Nature* 2011;476:220–223.

28 Hong JY, Lee SH, Lee SC et al. Therapeutic potential of induced neural stem cells for spinal cord injury. *J Biol Chem* 2014;289:32512–32525.

29 Khazaei M, Ahuja CS, Fehlings MG. Generation of oligodendrogenic spinal neural progenitor cells from human induced pluripotent stem cells. *Curr Protoc Stem Cell Biol* 2017;42:2D.20.1–2D.20.14.

30 Chambers SM, Fasano CA, Papapetrou EP et al. Highly efficient neural conversion of human ES and iPSC cells by dual inhibition of SMAD signaling. *Nat Biotechnol* 2009;27:275–280.

31 Karimi-Abdolrezaee S, Eftekharpour E, Wang J et al. Delayed transplantation of adult neural precursor cells promotes remyelination and functional neurological recovery after spinal cord injury. *J Neurosci* 2006;26:3377–3389.

32 Nguyen DH, Cho N, Satkunendrarajah K et al. Immunoglobulin G (IgG) attenuates neuroinflammation and improves neurobehavioral recovery after cervical spinal cord injury. *J Neuroinflammation* 2012;9:224.

33 Shibata S, Murota Y, Nishimoto Y et al. Immuno-electron microscopy and electron microscopic in situ hybridization for visualizing piRNA biogenesis bodies in drosophila ovaries. *Methods Mol Biol* 2015;1328:163–178.

34 Basso DM, Beattie MS, Bresnahan JC. A sensitive and reliable locomotor rating scale for open field testing in rats. *J Neurotrauma* 1995;12:1–21.

35 Le Dréau G, Martí E. Dorsal-ventral patterning of the neural tube: A tale of three signals. *Dev Neurobiol* 2012;72:1471–1481.

36 Wilson L, Maden M. The mechanisms of dorsoventral patterning in the vertebrate neural tube. *Dev Biol* 2005;282:1–13.

37 Fasano CA, Chambers SM, Lee G et al. Efficient derivation of functional floor plate tissue from human embryonic stem cells. *Cell Stem Cell* 2010;6:336–347.

38 Piper M, Barry G, Hawkins J et al. NFIA controls telencephalic progenitor cell differentiation through repression of the notch effector Hes1. *J Neurosci* 2010;30:9127–9139.

39 Yang H. Endogenous neurogenesis replaces oligodendrocytes and astrocytes after primate spinal cord injury. *J Neurosci* 2006;26:2157–2166.

40 Cloutier F, Siegenthaler MM, Nistor G et al. Transplantation of human embryonic stem cell-derived oligodendrocyte progenitors into rat spinal cord injuries does not cause harm. *Regen Med* 2006;1:469–479.

41 All AH, Gharibani P, Gupta S et al. Early intervention for spinal cord injury with human induced pluripotent stem cells oligodendrocyte progenitors. *PLoS One* 2015;10:e0116933.

42 Kawabata S, Takano M, Numasawa-Kuroiwa Y et al. Grafted human iPSC cell-derived oligodendrocyte precursor cells contribute to robust remyelination of demyelinated axons after spinal cord injury. *Stem Cell Rep* 2016;6:1–8.

43 Keirstead HS, Nistor G, Bernai G et al. Human embryonic stem cell-derived oligodendrocyte progenitor cell transplants remyelinate and restore locomotion after spinal cord injury. *J Neurosci* 2005;25:4694–4705.

44 Rosa PM, Martins LAM, Souza DO et al. Glioprotective effect of resveratrol: An emerging therapeutic role for oligodendroglial cells. *Mol Neurobiol* 2018;55:2967–2978.

45 Bankston AN, Mandler MD, Feng Y. Oligodendroglia and neurotrophic factors in neurodegeneration. *Neurosci Bull* 2013;29:216–228.

46 Shahbazi E, Mirakhori F, Ezzatizadeh V et al. Reprogramming of somatic cells to induced neural stem cells. *Methods* 2017;133:21–28. <https://doi.org/10.1016/j.ymeth.2017.09.007>.

47 Nishimura S, Sasaki T, Shimizu A et al. Global gene expression analysis following spinal cord injury in non-human primates. *Exp Neurol* 2014;261:171–179.

48 Hofstetter CP, Holmstrom NA, Lilja JA et al. Allodynia limits the usefulness of intraspinal neural stem cell grafts; directed differentiation improves outcome. *Nat Neurosci* 2005;8:346–353.

49 Kwon BK, Okon EB, Tsai E et al. A grading system to evaluate objectively the strength of pre-clinical data of acute neuroprotective therapies for clinical translation in spinal cord injury. *J Neurotrauma* 2011;28:1525–1543.

50 Pomeschchik Y, Puttonen KA, Kidin I et al. Transplanted human induced pluripotent stem cell-derived neural progenitor cells do not promote functional recovery of pharmacologically immunosuppressed mice with contusion spinal cord injury. *Cell Transplant* 2015;24:1799–1812.

51 Suzuki H, Ahuja CS, Salewski RP et al. Neural stem cell mediated recovery is enhanced by Chondroitinase ABC pretreatment in chronic cervical spinal cord injury. *PLoS One* 2017;12:e0182339.

52 Sekhon LH, Fehlings MG. Epidemiology, demographics, and pathophysiology of acute spinal cord injury. *Spine* 2001;26:S2–S12.



See www.StemCellsTM.com for supporting information available online.